Triple-gap superconductivity of MgB_2-(La,Sr)MnO_3 composite

V. N. Krivoruchko and V. Yu. Tarenkov

Donetsk Physics & Technology Institute NAS of the Ukraine, R. Luxemburg Street, 72, 83114 Donetsk, Ukraine

(Received 19 October 2011; revised manuscript received 12 July 2012; published 4 September 2012)

The interplay of superconductivity and magnetism was studied in a composite prepared from ferromagnetic half-metallic $La_{0.67}Sr_{0.33}MnO_3$ (LSMO) nanoparticles and the s-wave superconductor MgB_2. A few principal effects have been found. With the onset of MgB_2 superconductivity, a spectacular drop of the sample resistance was detected and complete superconductivity was observed at temperatures up to 20 K. The basic nanocomposite characteristics (critical temperature, current-voltage dependence, percolation threshold, etc.) are strongly affected by the half-metallic LSMO and, most probably, cannot be quantitatively explained within the framework of a conventional percolation scenario. Point contact (PC) spectroscopy was used to measure directly the superconducting energy coupling. For small voltage, an excess current and doubling of the PC normal-state conductance were detected. Conductance peaks corresponding to three energy gaps are clearly observed. Two of these gaps we identified as enhanced Δ_π and Δ_σ gaps originating from the MgB_2; the third gap Δ_{tr} is more than three times larger than the largest MgB_2 gap. The temperature behavior of Δ_{tr} does not follow the BCS dependence. The experimental results have a natural and qualitative explanation within the phase-coherency scenario of proximity-induced superconductivity. Specifically, at low temperature, a p-wave spin-triplet condensate with pairing energy Δ_{tr} is essentially sustained in LSMO but is incapable of displaying a long-range superconducting response because of a phase-disordered state. The proximity coupling to MgB_2 restores the long-range phase coherency of the superconducting state, which, in turn, enhances the superconducting state of the MgB_2.

DOI: 10.1103/PhysRevB.86.104502 PACS number(s): 74.45.+c, 74.40.−n, 74.78.Fk

I. INTRODUCTION

When a metallic ferromagnet (F) is in contact with an s-wave superconductor (SC), superconductivity is expected to decay rapidly (within a few nanometers) inside the F owing to the incompatible nature of superconductivity and ferromagnetic order.[1] This expectation was indeed confirmed in various materials and geometries. On the other hand, an increasing number of experimental facts[2–11] present clear evidence that a simple physical interpretation of the proximity effect, that the Cooper pairs are broken by a strong exchange field in the F layer, is in reality too simplistic, and an extension of the existing concepts of the interplay between superconductivity and ferromagnetism is needed. Long-ranged proximity effects have been observed in a variety of ferromagnetic materials, including wires,[2,3] bi- and multilayers,[4,10] half-metallic CrO_2,[7] rare-earth metals with helical magnetic structure,[6] etc.

From the theoretical viewpoint, a hybrid system of a F with a uniform exchange field in metallic contact with a SC is well understood, and the proximity effect may be described by taking into account the splitting of electronic bands of opposite spins.[1] The situation becomes more complicated if the magnetic structure is inhomogeneous. Theories[12–14] predict the appearance of a long-range proximity effect if there is a spatial variation of the magnetization in the F layer. In this case, the triplet component of anomalous correlations needs to be taken into consideration with a characteristic coherence length of $\xi_F = (D_F/2\pi T)^{1/2}$ that can be as large as ∼100 nm at low temperatures (here D_F is the diffusivity of the F metal and T is the temperature; we choose $\hbar = k_B = 1$). Thus, theoretical analysis of superconducting correlations in the presence of an inhomogeneous magnetic structure becomes nontrivial. In general, three different regimes may be distinguished: the magnetic disorder length is shorter than the Fermi wavelength (pointlike impurities), the disorder length is longer than the superconducting coherence length ξ_S (long-range disorder), and the magnetic disorder length is of the order of the coherence length ξ_S (medium-range disorder). In the medium-range regime, the role of magnetic disorder in superconducting proximity systems becomes nonlocal and nonuniversal (see, e.g., the discussion in Ref. 15 and references therein).

Magnetic inhomogeneities may in principle be artificially generated in ferromagnets. Yet existing technology cannot create them in a controlled way at the SC/F interface with nanoscale precision so that the most realistic scenario is to use a ferromagnet with given magnetic inhomogeneity. An interesting limit of heterostructured systems with tunable inhomogeneity of the magnetic partner is represented by SC/F nanocomposites. Being an experimentally accessible electronic system with controllable parameters, such heterostructures offer a unique testing ground for studying superconducting proximity systems with an arbitrary length of magnetic disorder. Superconductivity in granular mixture of superconductor-insulator films has been extensively studied, both experimentally and theoretically, in the framework of the percolation theory (see, e.g., Ref. 16). The proximity effects in granular-superconductor–normal-metal structures are also explored.[17,18] Yet we know of no reports addressing proximity effects in composites of a (nano)granular half-metal ferromagnet (HMF) and a conventional s-wave superconductor.

Another topic of fundamental interest today is spatial inhomogeneity in the superconducting density of states and the superconducting state, which is governed by quantum phase fluctuations.[19–22] In most mean-field theories it is suggested that the relation $T_\varphi > T_\Delta$ is fulfilled between the temperatures of electron pairing T_Δ and the long-range phase coherency T_φ. This means that global phase coherency and the energy gap appear (vanish) at the same temperature,

mainly due to the opening (disappearing) of the gap with temperature. However, it has been shown[19] (see also Refs. 20 and 21) that for systems with low conductivity and small superfluid density (bad metals), the temperature of the global phase coherency T_φ is reduced significantly and becomes comparable to or even smaller than the pairing temperature T_Δ. In this case, the critical temperature T_C is determined by the global phase coherency, whereas a local pair condensate could exist well above T_C. In particular, for high-T_C cuprates diamagnetism due to fluctuating superconducting pairs above the superconducting transition temperature as well as the origin of the so-called pseudogap still remain under active discussion (see, e.g., Refs. 23–28 and references therein).

In our recent works anomalous superconductivity has been detected in point contacts (PCs) of half-metallic manganite (La,Sr)MnO_3 and (La,Ca)MnO_3 with an s-wave SC, Pb or MgB_2.[29,30] In particular, for proximity-affected PCs, coherent multiple Andreev reflection (subharmonic gap resonances) has been observed, and it has been found that the proximity-induced superconducting gap of (La,Sr)MnO_3 or (La,Ca)MnO_3 is much larger than that of Pb or MgB_2. It was implied that, at low temperature, *incoherent superconducting fluctuations are essentially sustained in half-metallic manganites and, in the proximity-affected region, the singlet superconductor establishes phase coherence in the p-wave spin-triplet superconducting state of the manganites*.[29,30] To verify this phase-disordering scenario for the anomalous superconductivity of proximity-affected PCs, we prepared and systematically studied the normal and superconducting properties of an MgB_2–(nano) $La_{0.67}Sr_{0.33}MnO_3$ (MgB:LSMO) composite. The key idea was to obtain a composite where proximity-affected HMF/SC interfaces govern the superconducting properties of the bulk sample. Fortunately, the idea was successful: the bulk samples of the MgB:LSMO (nano)composite demonstrate direct evidence for unconventional superconductivity with large, up to 20 K, critical temperature T_C. In this paper we present the results of an investigation of the superconducting properties of such systems.

To directly measure the superconducting energy coupling, the point-contact spectroscopy technique has been used.[31] In particular, a study of the current-voltage characteristics and of the dynamic conductance of PCs between the MgB:LSMO composite and different metallic needles (In, Ag, Nb, and $La_{0.65}Ca_{0.35}MnO_3$) has been performed. Our key findings are as follows: Three superconducting gaps are clearly observed. We identified two of these gaps as *enhanced* MgB_2 gaps, while the third quasiparticle gap Δ_{tr} cannot be attributed to this superconductor. The magnitude of Δ_{tr} is more than three times larger than the largest MgB_2 gap and is the same as earlier detected in Refs. 29 and 30. Also, we found that all the energy gaps vanish simultaneously as the temperature increases towards T_C of MgB_2. Yet the temperature behavior of Δ_{tr} does not correspond to the BCS dependence. The data obtained on the contacts with $La_{0.65}Ca_{0.35}MnO_3$ give additional arguments in favor of a spin-polarized supercurrent in the composite.

The origin of the large quasiparticle gap Δ_{tr} and the enhancement of the MgB_2 gaps cannot be explained on the basis of the existing theoretical models. We believe the results obtained indicate a type of superconducting proximity effect which follows the scenario of a "latent" high-T_C superconductivity in doped manganites as suggested in Refs. 29 and 30. That is, MgB_2 enhances the internal superconducting order parameter phase stiffness in LSMO and, in turn, being in the superconducting state, LSMO enhances the superconducting characteristics of MgB_2. Taking into account the half-metallic properties of LSMO, the Curie temperature (i.e., the exchange field) magnitude, as well as data documented on PCs between composite and half-metallic manganite, it is likely that in the case of LSMO we deal with even-requency p-wave spin-triplet superconducting pairing.

The structure of the paper is as follows. Section II is devoted to the sample preparation and experimental details. Section III is the central one; here we present our experimental results on the superconducting characteristics for bulk samples and point contacts. We start Sec. IV by summarizing the main experimental facts, and then we discuss our speculations about a possible scenario explaining the observations. In Sec. V we summarize the results and formulate the main conclusions. This report may be considered as the next step in our efforts[29,30] to understand the phenomenon of the mutual influence of singlet s-wave superconducting pairing and the non-Fermi half-metallic ferromagnetic state of doped manganites.

II. SAMPLES AND EXPERIMENTAL DETAILS

Stoichiometric MgB_2 has a transition temperature $T_{C0} =$ 39 K, the highest among conventional superconductors.[32] MgB_2, however, is by no means an ordinary superconductor, but a superconducter with weakly interacting multiple bands (two bands, σ and π). It demonstrates distinct multiple superconducting energy gaps (the σ and π gaps) with energy $\Delta_\pi = 2.3$ meV and $\Delta_\sigma = 7.1$ meV at $T = 4.2$ K.[32] The coherence length ξ_S is anisotropic with $\xi_{ab}(0) \approx 8$ nm and $\xi_c(0) \approx 2$ nm.[32] $La_{0.67}Sr_{0.33}MnO_3$ is a HMF with $T_{\text{Curie}} =$ 320 K (see, e.g., Ref. 33). In this work, composites containing submicron MgB_2 powder and LSMO nanoparticles (about 20–30 nm in size) have been produced. Details of the LSMO nanoparticle preparation can be found in Ref. 34. Comparative investigations of the nuclear magnetic resonance and nuclear spin-spin relaxation of ^{55}Mn nuclei of nanopowders and polycrystalline samples with the same composition confirmed the presence of the ferromagnetic metallic state and phase separation, which is typical for manganites, for particles of the size we used.[35]

Powders with different weight ratios of LSMO and MgB_2 were mixed and pressed (under pressure up to 60 kbars) in stripes, and a number of samples of different composition were obtained. Note that compared with high-temperature superconducting oxides, obvious properties of MgB_2 include transparent boundaries without weak links, high carrier density, high energy gaps, strong links among grains, etc. (see, e.g., Refs. 36 and 37 and references therein). There is not much influence on the MgB_2 superconductivity when a sample is contaminated or doped at a small ratio.

The composites obtained were analyzed by the method of x-ray energy-dispersive spectroscopy (EDX) using an INCAPentaFETx3 spectrometer and a JSM-6490LV scanning

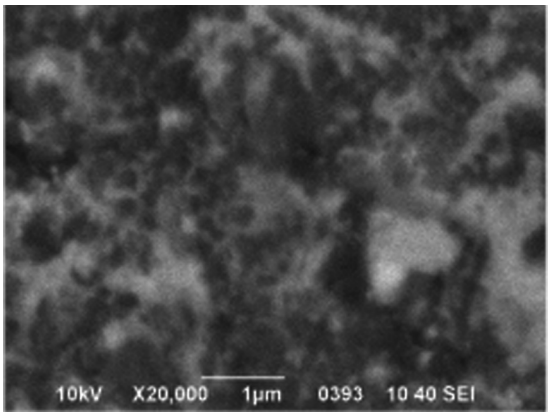

FIG. 1. SEM image of MgB_2:$La_{0.67}Sr_{0.33}MnO_3$ composite with 3:1 weight ratio (black, MgB_2; light tone, $La_{0.67}Sr_{0.33}MnO_3$).

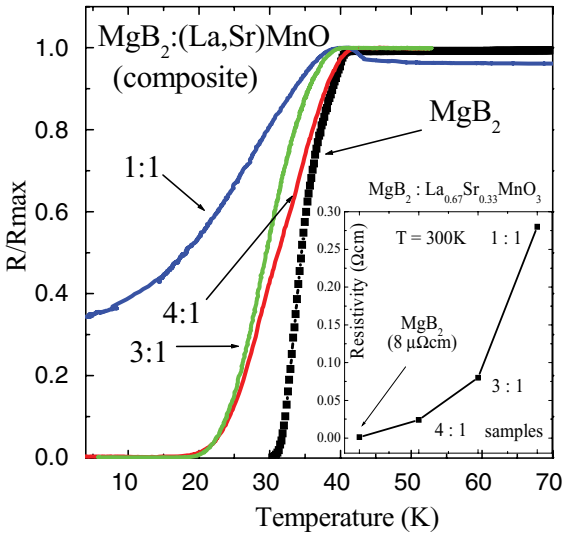

FIG. 2. (Color online) Temperature dependence of the normalized resistivity $R(T)/R(T = 39\ \text{K})$ of the samples of MgB_2:$La_{0.67}Sr_{0.33}MnO_3$ with weight ratios 1:1, 3:1, and 4:1, as well as of pure (weight ratio 1:0) compacted MgB_2. Inset: the sample resistivity at $T = 300$ K.

electron microscope (SEM). As an example, one of the sample's SEM micrographs is shown in Fig. 1. Magnetic properties were measured with a commercial cryostat system (PPMS-9). In all transport measurements the standard four-point configuration with the low-frequency ac technique was used. The resistance was measured with a current of $\sim 50\ \mu$A. For samples of the same (nominal) composition, sample-to-sample fluctuations in magnitude of the critical temperature and the critical current were detected. A weak hysteretic behavior reflecting the magnetic subsystem's prehistory dependence was also observed.

Metallic contacts between the composite plate and a tip were formed by pressing a needle-shaped wire against the polished composite's surface. The contacts were made at room temperature and at liquid-nitrogen temperature as well, but the results did not depend upon the method of preparation. The contact parameters were stable, offering the possibility of performing measurements in a wide temperature range. The transition resistance of the current and potential contacts was $R \sim 10^{-8}\ \Omega\,\text{cm}^2$. The junctions' resistance was much larger ($\sim$1–30 Ω), so that the rescaling effects can be neglected. The analysis showed that we deal with the so-called Sharvin contacts[38] and the contact's transport regime corresponds to the intermediate regime, i.e., is neither ballistic nor diffusive (for more details see Ref. 39). The PCs' conductance dI/dV-V spectra, which reflect the local density of states, were numerically derived from the current-voltage (I-V) curves.

III. EXPERIMENTAL RESULTS

A. Bulk characteristics

Representative temperature dependences of the normalized resistivity $R(T)/R(T = 39\ \text{K})$ of the (bulk) samples with MgB_2:$La_{0.67}Sr_{0.33}MnO_3$ weight ratios 1:1, 3:1, and 4:1, as well as of the MgB_2 sample without manganite, are shown in Fig. 2 (main panel). According to the $R(T)$ dependences, below the superconducting transition temperature of MgB_2, the resistivity of the samples 3:1 and 4:1 sharply decreases. The midpoint and complete (T_C) superconducting transition temperatures were determined from the $R(T)$ behavior as 30 and 20 K, respectively. The resistivity of the sample 1:1 also decreases, but the compound of this composition still remains in a resistive state down to the lowest temperature 4.2 K. Sometimes a hysteretic shift in $R(T)$ behavior reflecting the (magnetic) prehistory dependence of the transition temperature was also detected. Below $T_C = 20$ K, the characteristics of the sample 4:1 basically reproduce those for the composition 3:1, and in what follows we concentrate on the results obtained for the samples with weight ratio 3:1.

Figure 3 (main panel) shows the current-voltage characteristic of the sample 3:1, taken at 4.2 K. We observe a clear

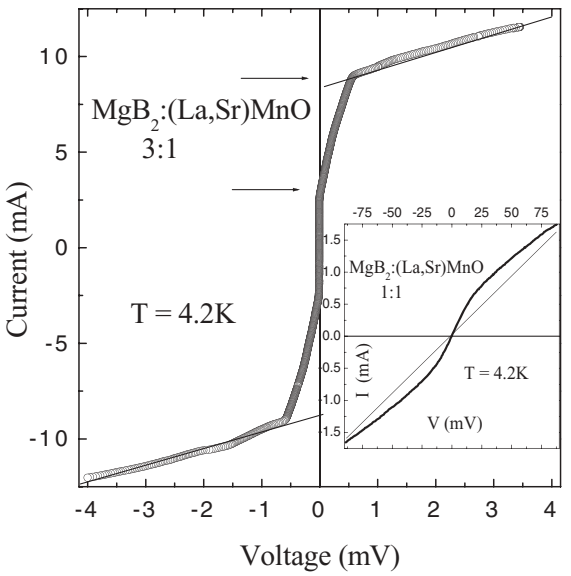

FIG. 3. Current-voltage characteristic of MgB_2:$La_{0.67}Sr_{0.33}MnO_3$ (3:1) sample. Inset: the same for the MgB_2:$La_{0.67}Sr_{0.33}MnO_3$ (1:1) sample.

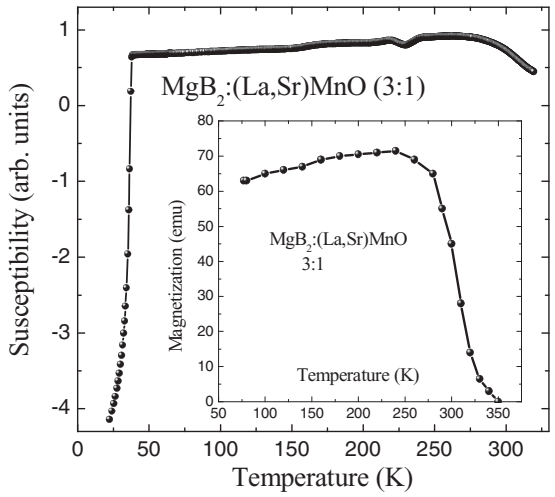

FIG. 4. Temperature dependence of the magnetic susceptibility of MgB_2:$La_{0.67}Sr_{0.33}MnO_3$ (3:1) sample. Inset: magnetization in high-temperature region.

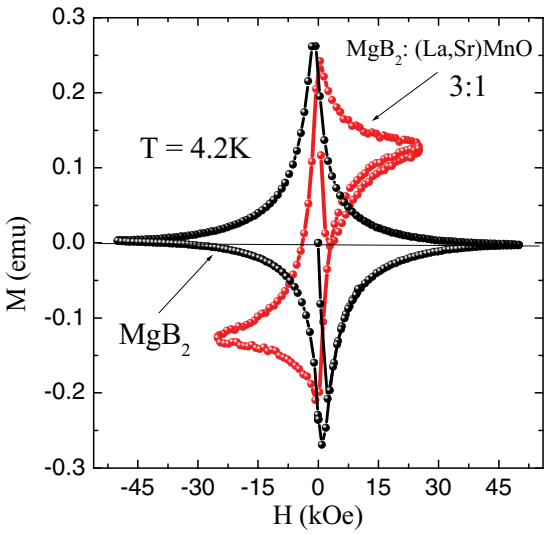

FIG. 5. (Color online) Magnetization $M(H)$ curves of the MgB_2:$La_{0.67}Sr_{0.33}MnO_3$ (3:1) sample and compacted MgB_2; $T = 4.2$ K.

zero-resistance supercurrent branch, with a maximum value for I_C of 2.5 mA. From the *I-V* curves the critical current I_C of the composite was determined as the first deviation from a vertical line around zero bias. The second deviation from linearity around 0.6 mV bias, with a maximum value of 8.9 mA, is attributed to the critical current of the MgB_2 powder. In the current interval $2.5 < I < 8.9$ mA, the sample is in a resistive state and could be considered as a system of small superconductive islands within a normal matrix. For comparison, the *I-V* characteristic of the sample 1:1 at 4.2 K is also shown in Fig. 3 (inset). This system remains in a resistive state; however, as for the 3:1 sample, an excess current has been clearly observed; i.e., the MgB_2 grains stay in a superconducting state. Formally, the system is similar to arrays of resistively shunted Josephson junctions.

The magnetic susceptibility $\chi(T)$ and magnetization $M(T)$ of the 3:1 compound plotted for different temperatures are shown in Fig. 4 (main panel and inset, respectively). It is possible to see, with decreasing temperature, a transition into a ferromagnetic state occurring at $T_{\text{Curie}} \approx 320$ K, and then, below 39 K, a diamagnetic response is developed. The measured magnetization hysteresis loops $M(H)$ for the compacted MgB_2 and sample 3:1 are illustrated in Fig. 5. For the composite, note the nonzero value of $M(H = 0)$ for the initial branch of the magnetization curve. This shift in $M(H)$ is directly related to the already mentioned magnetic prehistory of the sample. These data provide unambiguous evidence that the composite is a type-II superconductor with a strong vortex pinning.

As already mentioned in the Introduction, the superconductivity in bulk composite systems has been extensively studied within the percolation scenario.[16–18] It has been established that when the size of grains of the superconducting material, d, is large enough, $d \gg \xi_S$, their basic intragranular characteristics (critical temperature, gap value, etc.) are not affected by the proximity of the nonsuperconducting component and remain close to the bulk value both above and below the percolation threshold. For these systems, the macroscopic transition temperature can be reduced due to suppression of the intergranular coupling. However, if a typical grain size is smaller than the coherence length, $d \ll \xi_S$, the basic intragranular characteristics are strongly affected by the presence of the normal metal due to the proximity effect. For such systems the macroscopic transition temperature will be reduced due to both the proximity effect and the quality of the intergranular coupling.[17,18]

For a three-dimensional sample the percolation theory predicts $f_C = 0.16 \pm 0.02$, where f_C stands for the percolation threshold of the volume fraction of the superconducting component, f, in the three-dimensional lattice percolation model [i.e., f_C is the percolation threshold of grains with linear dimension $\sim\xi_S$ (Ref. 18)]. Thus, for the composite systems under consideration, the grains of the superconducting material, MgB_2, are large enough, i.e., $d \gg \xi_S$, and below the percolation threshold the macroscopic transition temperature T_C should not be strongly dependent on composition variation over a wide range. However, as seen in Fig. 2, for the sample 1:1 with volume fraction about $f = 0.33$, i.e., about two times larger than f_C, there is no transition into the superconducting state. Moreover, the T_C is strongly reduced from the compacted (weight ratio 1:0) MgB_2 value $T_{C0} = 30$ K even at concentrations when an infinite cluster of MgB_2 percolating from one side of the sample to the other is sure to exist: see the $R(T)$ data in Fig. 2 for the 3:1 and 4:1 samples. There are no reasons to expect a critical temperature reduction due to the intergranular coupling because, as is well established, MgB_2 is characterized by transparent boundaries without a weak-link problem.[36,37]

Thus, the bulk sample behaviors indicate that the conventional percolation scenario, most probably, does not apply here. To obtain additional arguments for or against this conclusion, we perform comparative investigations on bulk samples of submicron MgB_2 and nanoparticles (about 10 nm) of magnetite Fe_3O_4. Magnetite is a ferrimagnet with an anomalously high Curie temperature $\sim$850 K. Band-structure calculations (see, e.g., Ref. 40) have predicted that Fe_3O_4 is

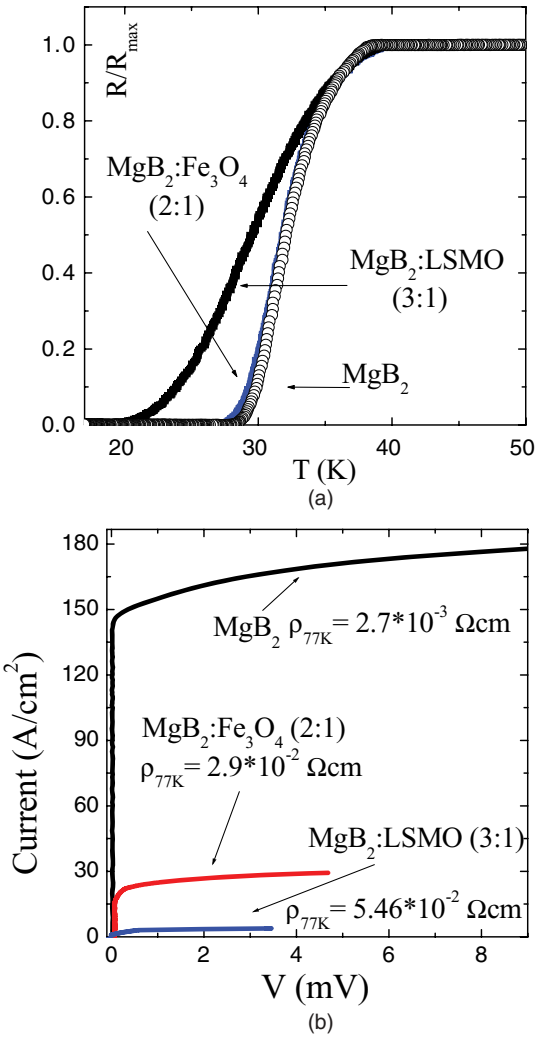

FIG. 6. (Color online) (a) Temperature dependence of the normalized resistivity $R(T)/R(T = 39\ \mathrm{K})$, and (b) current-voltage characteristic of the samples of MgB_2:$La_{0.67}Sr_{0.33}MnO_3$ with weight ratio 3:1 and MgB_2:Fe_3O_4 with weight ratio 2:1, as well as of pure (weight ratio 1:0) compacted MgB_2; $T = 4.2$ K.

a half metal with only one spin subband at the Fermi level. Experimentally, spin-resolved photoemission on epitaxial thin films indeed indicated a spin polarization of about 80% at room temperature.[41] However, below a Verwey transition at about 120 K, single-crystal Fe_3O_4 shows a nonmetallic (polaronic) type of conductivity (see, e.g., Ref. 42). For our measurements, the samples with different weight ratios of Fe_3O_4 and MgB_2 were prepared in a mode similar to that used for the samples with manganites.

Figure 6(a) shows the temperature dependences of the normalized resistivity $R(T)/R(T = 39\ \mathrm{K})$ of three representative samples: the MgB:LaSrMnO with weight ratio 3:1, the MgB_2:Fe_3O_4 with weight ratio 2:1, and the compacted MgB_2 sample. According to the $R(T)$ dependences, the critical temperature of the MgB_2:Fe_3O_4 (2:1) composite is not affected by the proximity of the nonsuperconducting component and remains close to that of the compacted MgB_2 system. That is what one would expect, in accordance with conventional percolation physics, for a system above the percolation threshold. Figure 6(b) shows the current-voltage characteristic of these three samples, taken at 4.2 K. For all systems we observe a clear zero-resistance supercurrent branch, but with a maximum value for I_C different by orders of magnitude [about two orders between MgB:LaSrMnO (3:1) and MgB_2]. Again, we see that the characteristics of the system with manganite do not follow the conventional percolation scenario, while for the system with magnetite they do.

The quantitative analysis of the results illustrated in Figs. 2–6 is quite complex and will be carried out elsewhere. We summarize here that predictions based on conventional percolation physics do not work for MgB:LSMO nanocomposites; the basic system's characteristics are strongly affected by the ferromagnetic manganite due, most probably, to an unconventional proximity effect. This hypothesis will find further confirmation in the point contact spectroscopy measurements.

To finish this section, let us note that much earlier Kasai *et al.* investigated the current-voltage characteristics of YBCO/$La_{1-x}Ca_xMnO_z$/YBCO (Ref. 43) and YBCO/$La_{1-x}Sr_xMnO_z$/YBCO (Ref. 44) layered junctions (here YBCO stands for $YBa_2Cu_3O_y$). Surprisingly, a supercurrent was observed through magnetic barriers as thick as 500 nm for junctions with $La_{1-x}Ca_xMnO_z$ and 200 nm for junctions with $La_{1-x}Sr_xMnO_z$, that is, for barriers thicknesses much larger than one can expect based on the conventional proximity effect. Yet this phenomenon occurred only for manganese oxides with $x = 0.3$–0.4. The authors suggested that the results may be due to a novel proximity effect between YBCO and doped manganites. To the best of our knowledge, so far the observations of Refs. 43 and 44 have not been reasonably explained, and the hypothesis has been neither proved nor disproved. These experimental results, in our opinion, strongly support our statement about unconventional superconducting proximity effect in manganites.

B. Point contact spectra

The method of Andreev reflection spectroscopy is a direct and sensitive method of studying such microscopic characteristics of superconductors as the density of quasiparticle states, the value of the superconducting gap, the symmetry of the superconducting pairing, etc. We used the point contact technique to measure directly the energy of superconducting pairing in the heterostructures under consideration.[31]

Figure 7 shows representative dynamic conductance spectra $dI/dV = G(V)$ of microconstrictions between In, Ag, and Nb tips and the sample 3:1 (a configuration commonly called the "needle anvil") measured at $T = 4.2$ K. At low voltage, conductance peaks corresponding to three superconducting gaps with energies $\Delta_1(\pi) = 2.0$–2.4 meV, $\Delta_2(\sigma) = 8.4$–11.7 meV, and $\Delta_{\mathrm{tr}} = 19.8$–$22.4$ meV are clearly observed. (Further on, we simply denote by Δ the position of the dI/dV minimum. For PCs with a not too large Γ parameter, introduced by Dynes *et al.*,[45] this value does not differ too much from the true energy gap.) Two of these gaps, $\Delta_1(\pi)$ and $\Delta_2(\sigma)$, we recognize as enhanced MgB_2 gaps, i.e., as originating (most probably) from the Δ_π and Δ_σ gaps of MgB_2, respectively. [Note, to avoid confusion, that within experimental uncertainty, the magnitude of the smallest $\Delta_1(\pi)$ gap still remains in range of the bulk MgB_2 gap.[32] A possible explanation of this behavior

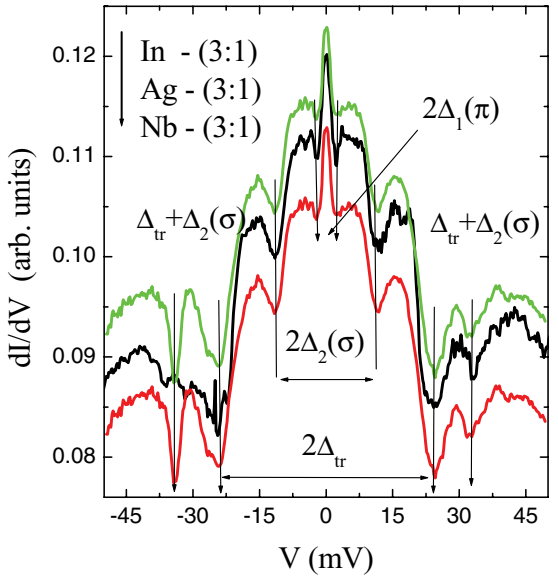

FIG. 7. (Color online) The Andreev reflection spectra of In, sample 3:1, Ag, sample 3:1, and Nb, sample 3:1 point contacts.

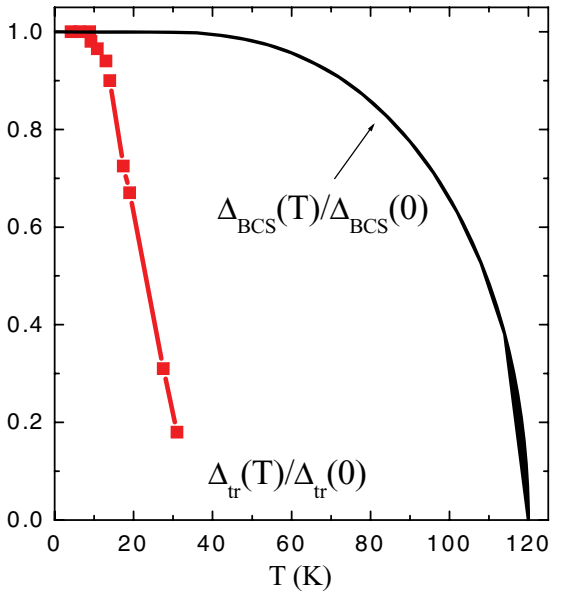

FIG. 8. (Color online) Gap $\Delta_{tr}(T)$ values (relative to the zero-temperature gap) of the MgB_2:$La_{0.67}Sr_{0.33}MnO_3$ (3:1) composite as a function of temperature and the BCS gap temperature dependence.

is that the σ- and π-band orbitals, having different parity, are orthogonal in coordinate space, and interband transitions are rare enough.[46]] The third gap, Δ_{tr}, we attribute (see the discussion below) to the intrinsic superconducting pairing in LSMO. It is worth underlining here that the magnitude of Δ_{tr} is the same as those earlier detected in PCs of (La,Sr)MnO_3 and (La,Ca)MnO_3 with Pb or MgB_2.[29,30] Note that the PCs' resistivity varied by orders of magnitude, but the multiple-gap structure in the quasiparticle density of states of the composite, as well as the gap energy magnitudes, were robust features of the superconducting composites and were reproduced in all PCs we prepared.

We detected that all the energy gaps vanish simultaneously as the temperature increases towards T_C of MgB_2. In Fig. 8, the temperature dependence of the energy gap Δ_{tr} is shown. From the BCS relation $\Delta(0) = 1.76k_BT_C$, the $\Delta_{tr}(0)$ gap would lead to a superconducting state with $T_C \approx 120$ K. The classic BCS gap temperature behavior is shown in the figure, too. As is evident, the experimental behavior of $\Delta_{tr}(T)$ does not follow the BCS dependence. In fact, the temperature dependence of the largest gap detected, $\Delta_{tr}(T)$, directly proves that its existence is not an "independent" property but is due to the superconducting state of MgB_2, i.e., it is due to some kind of proximity effect.

Having suggested the possibility of a spin-triplet proximity-induced superconducting state in doped manganites, it is reasonable to try to reveal the supercurrent spin polarization. Let us recall here that, at energies below the superconducting gap, a charge transport through a normal nonmagnetic (N) metal in contact with a SC is possible only due to a specific process called Andreev reflection (AR),[47] a two-particle process in which, in the N metal, an incident electron above the Fermi energy E_F and an electron below E_F with the opposite spin are coupled together and transferred across the interface into the SC side, forming a Cooper pair in the condensate. Simultaneously, an evanescent hole with opposite momentum and spin appears in the N metal. The charge doubling at the interface enhances the subgap conductance,[48,49] and this phenomenon has indeed been observed in the case of a perfectly transparent interface. The picture is significantly modified when spin comes into play. In particular, if the N metal is a half-metallic ferromagnet, there is full imbalance between spin-up and spin-down populations, which suppresses the AR and reduces the subgap conductance to zero. This physics was our motivation to investigate the current-voltage characteristics of PCs between the sample 3:1 and another half-metallic manganite, $La_{0.65}Ca_{0.35}MnO_3$ (LCMO). Indeed, according to the existing publications,[50] including our earlier measurements,[39] the charge carrier polarization for LCMO is large, greater than 75%. Thus, if a supercurrent in the composite is unpolarized [an s-wave or a p-wave ($S = 1, m = 0$) component of triplet pairing] the AR will be suppressed and the subgap conductance will be reduced below the normal-state value. On the contrary, if at both sides of the contact the charge current is spin polarized, there is no restriction (because of spin) on the AR and, as in the conventional case,[48,49] an excess current and a doubling of the normal-state conductance are observed.

In Fig. 9 we documented the current-voltage, Fig. 9(a), and the AR spectra, Fig. 9(b), of two representative PCs of the composite (3:1) and LCMO. Note that the normal-state resistivity of these contacts differs by about factor of 3, yet the contacts demonstrate common specific features. Namely, at low voltage, an excess current is unambiguously detected; the conductance spectra are practically identical and reproduce all the principal features of the system that have been detected for PCs with In, Ag, and Nb: the enhanced gap Δ_σ and the value of Δ_{tr}, in particular. Also, as in the cases shown in Fig. 9(b), for all investigated contacts almost a doubling of the normal-state conductivity has been observed. [An interesting feature which characterizes the data in Fig. 9(b) is worthy of note. In the region of voltage $-\Delta_2(\sigma) < eV < \Delta_2(\sigma)$ the PC spectrum

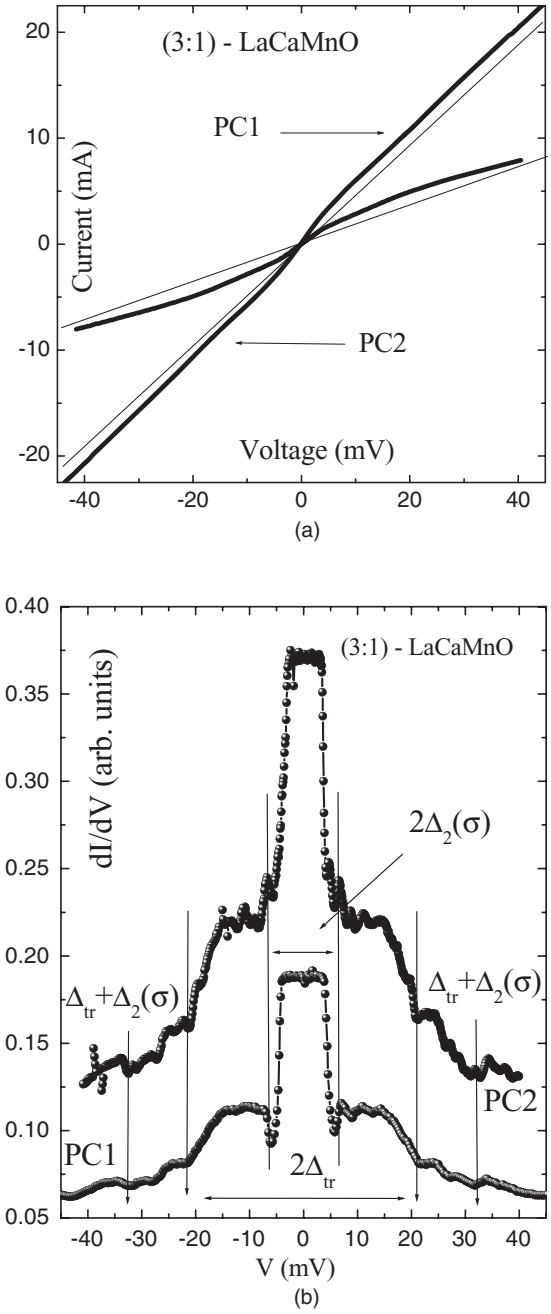

FIG. 9. The current-voltage (I-V) dependence (a) and the Andreev reflection spectra (b) of point contacts of the $La_{0.65}Ca_{0.35}MnO_3$ (3:1) composite.

coincides with a perfect one, i.e., as if we deal with the case of a fully transparent barrier between metals.] The data in Fig. 9 are an additional argument in favor of a spin-polarized supercurrent in the MgB:LSMO composite.

At the end of this section, let us consider the $eV > \Delta_{tr}$ region. Inspecting the data in Figs. 7 and 9(b) for different contacts, we find an additional dip at $eV \approx 31.8$–34.2 meV. To elucidate the origin of this dip, let us remember that an alternative but equivalent way of thinking about the proximity effect (or the microscopic origin of the proximity effect) is through the AR processes. According to contemporary models (see, for example, Refs. 51 and 52 and references therein), for SC_1-N-SC_2 weak links or short constrictions SC_1-c-SC_2 between two superconductors, the differential conductance dI/dV drops fairly abruptly due to multiple AR reflection (-c- stands for constriction). These conductance drops appear at voltages that correlate with the energy of quasiparticle gaps divided by integers. The voltages at which the conductance subharmonic structure appears (roughly, because the boundary conditions at SC-N or SC-c interfaces are also important[52]) are $eV_n = \Delta_1/n$, $eV_m = \Delta_2/m$, and $eV_l = (\Delta_1 + \Delta_2)/(2l + 1)$, where the integers (l,n,m) are restricted depending on the energy gap ratio (Δ_1/Δ_2). Whether a given conductance drop is present and its prominence depend on the energy gap ratio Δ_1/Δ_2, and for large differences between gaps, $\Delta_1 < 0.5\Delta_2$ only the integers $n > 0$, $l = 0$, and $m = 1$ are allowed. What is important for us here is that the resonances can be observed only if *both electrodes are superconductors*. There is no multiple AR when one of the electrodes is in a normal state.

Returning to the additional dip in Figs. 7 and 9(b), we found that this dip has a natural and quantitative explanation if we assign $\Delta_1 = \Delta_2(\sigma)$ (=8.4–11.7 meV) and $\Delta_2 = \Delta_{tr}$ (=19.8–22.4 meV). Note that we have not found any additional structure arising from multiple AR reflection and causing the conductance dips at "forbidden" $l \neq 0$. Thus, the observation of the conductance drop at $eV = [\Delta_{tr} + \Delta_2(\sigma)]$ is one more piece of evidence that LSMO is in a superconducting state. Simultaneously, this proves the fact that not the initial value of the gap Δ_σ but the enhanced $\Delta_2(\sigma)$ one is a *real gap in the quasiparticle spectrum* of the MgB_2 in the composite.

IV. DISCUSSION

Before we get into a qualitative explanation of the experimental results, let us summarize the main experimental anomalies that have been detected for the compounds under consideration. The following features have been detected for the bulk samples characteristics: (i) Superconductivity of the samples MgB:LSMO with 3:1 and 4:1 weight ratios with a midpoint transition at 30 K has been observed. (ii) The basic attributes (critical temperature, current-voltage dependence, percolation threshold, etc.), most probably, cannot be quantitatively explained within the framework of a conventional percolation scenario. Point contact spectroscopy documented the next peculiarities: (iii) Three distinct quasiparticle energy gaps $\Delta_1(\pi)$, $\Delta_2(\sigma)$, and Δ_{tr} are clearly revealed. Two of these gaps were identified as enhanced gaps originating from the MgB_2. (Note that this feature cannot be detected in the conventional point contact geometry.) The third gap, Δ_{tr}, was the same as those earlier detected in the PCs of $(La,Sr)MnO_3$ and $(La,Ca)MnO_3$ with Pb or MgB_2,[29,30] and thus could not be related to s-wave superconductivity. (iv) The temperature behavior of the Δ_{tr} gap does not follow the BCS dependence.

In our opinion, the origin of the large quasiparticle gap Δ_{tr} and enhancement of the largest MgB_2 gap Δ_σ cannot be explained on the basis of the existing theoretical models of the proximity effect. The observed anomalies have a natural and qualitative explanation within a scenario of a latent high-T_C superconductivity in doped manganites.[29,30]

Theoretically, the proximity effect in normal-metal–two-band hybrid structures has been considered by Brinkman *et al.*[53] A phenomenon was predicted in which the superconductivity in a two-band SC is enhanced by the proximity to a superconductor with a lower transition temperature (SC′). The physics of this effect is explained by the coupling between SC′ and the π band: the SC′ enhances the superconductivity in the (small) π band, whereas the π-σ interband coupling causes an enhancement of the superconductivity in the σ band. However, for the MgB:LSMO composite we found three quasiparticle gaps, the largest of which, $\Delta_{\rm tr}$, could not be attributed to MgB_2. Also, a substantial increase in the magnitude of the largest of the MgB_2 gaps, Δ_σ, has been detected. Thus, a question arises as to which of the observed gaps is proximity induced.

Before giving a qualitative explanation of the observations, we summarize the physics of the proximity effect at a spin-active HMF/SC interface, as follows (see, e.g., Ref. 14 and references therein). The conversion process between the singlet and equal-spin triplet supercurrents is believed to be governed by two important phenomena taking place in the half metal at the interface: (i) a spin mixing and (ii) a spin-rotation symmetry breaking. Spin mixing is the result of the different scattering phase shifts that electrons with opposite spin acquire when scattered (reflected or transmitted) from an interface.[54] It results from either a spin polarization of the interface potential, or differences in the wave-vector mismatches for spin-up and spin-down particles at either side of the interface, or both. It is a robust and ubiquitous feature for interfaces involving strongly spin-polarized ferromagnets.

Broken spin-rotation symmetry leads to spin-flip processes at the interfaces. Its origin depends on the microscopic magnetic state at the HMF/SC interface, the character of local magnetic moments coupling with itinerant electrons, etc., and even varies from sample to sample. However, the exact microscopic origin of spin-flip processes at the interface is important only for the effective interface scattering matrix[14] and not for superconducting phenomena, since Cooper pairs are of the size of the coherence length ξ_S, which is much larger than the atomic scale.

Due to spin mixing at the interfaces, a spin triplet ($S = 1$, $m = 0$) amplitude $f^{\rm tr}_{\uparrow\downarrow}(r) = (|\uparrow\downarrow\rangle + |\downarrow\uparrow\rangle)$ is created and extends from the interface for about the magnetic length $\xi_F = (D_F/2\pi H_{\rm exc})^{1/2}$ into the F layer ($H_{\rm exc}$ denotes the exchange field in the F). (In the case of a fully spin-polarized F the conversion of singlet pairs into triplet takes place entirely within the singlet SC.[14]) At the same time, triplet pairing correlations with equal spin pairs ($S = 1, m = +1$ or $m = -1$) are also induced (due to spin-flip processes) in the F layer. These components decay on the thermal length scale $\xi_T = (D_F/2\pi T)^{1/2}$ which is much larger than ξ_F because in typical cases the exchange field $H_{\rm exc}$ is much larger than T_C. It is worthy of emphasis that it is only the $m = 0$ triplet component that is coupled via the spin-active boundary condition to the equal-spin $m = 1$ pairing amplitudes in the half metal. The singlet component in the s-wave superconductor, $f^s_{\uparrow\downarrow}(r) = (|\uparrow\downarrow\rangle - |\downarrow\uparrow\rangle)$, being invariant under rotations around any quantization axis, is not directly involved in the creation of the triplet $m = 1$ pairing amplitudes in the half metal.

Let us now proceed to our system. Within the double-exchange interaction model for hole-doped manganites, the itinerant charge carriers provide both the magnetic interaction between magnetic moments of the nearest Mn^{3+}-Mn^{4+} ions and the system's electrical conductivity. Also, several theoretical models and numerous experimental data suggest that atomic-scale nonhomogeneity is an intrinsic feature of these compounds surface (see, e.g., Ref. 33). Another characteristic important for our discussion is that, due to Hund's interaction (for Mn^{3+} the Hund's energy $\sim$1 eV), spin disorder serves as a strong spin-scattering center for charge carriers. Due to the short mean free path, which is typically of the order of the distance of about a lattice parameter, the charge carrier probes the magnetization on a very short length scale. At the interface with the superconductor, the local moments are expected to show a certain degree of disorder, and it is reasonable to expect that the interface ferromagnetic-manganite–s-wave-SC is a spin-active one. Following Refs. 29 and 30, we suggest that, at low temperature, a noncoherent p-wave even-frequency spin-triplet superconducting condensate already exists in half-metallic manganites. Being proximity coupled to the singlet SC, the $m = 0$ triplet component in the manganite is coupled via the boundary condition to the singlet pairing amplitude in the SC partner. At the same time, the spin-active boundary leads to coupling of the $m = 0$ triplet component with an equal-spin, $m = 1$, pairing amplitude in manganite. These couplings yield phase coherency of both the $m = 0$ and equal-spin $m = 1$ triplet Cooper pairs in the HMF with a large quasiparticle gap $\Delta_{\rm tr}$ ($>\Delta_\pi, \Delta_\sigma$). As an inverse effect, being proximity linked to the s-wave pairing amplitude, the $m = 0$ amplitude of the triplet superconducting state enhances the quasiparticle gap(s) of a singlet SC. Figure 10 illustrates the described mechanism of the long-range phase coherency due to the proximity effect in the nanocomposite. [Detailed discussion of the physics shown in Fig. 10 is given in Ref. 30(b) for proximity-affected PCs. Naturally, all arguments for a point contact geometry are preserved for the HMF/SC interface in the composite, and we refer the reader to Ref. 30(b).]

In mean-field BCS-Eliashberg theories with $\Delta(r) = |\Delta_{MF}(r)|e^{\varphi(r)}$, the characteristic energy scale responsible for the global transition temperature T_C is the superconducting

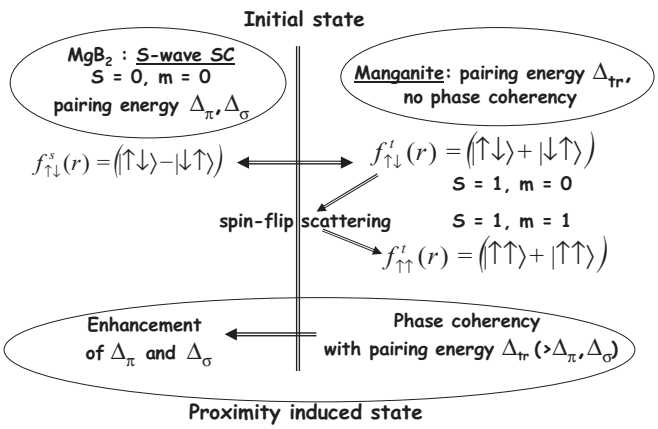

FIG. 10. A sketch of the long-range phase coherency due to the proximity effect in the composite.

energy gap $|\Delta_{MF}(r)|$. This implies that the spatial variation in $|\Delta_{MF}(r)|$ is small, and that the global phase coherence temperature T_φ is larger than (or equal to) T_C. However, for systems with small superfluid density the spatial variations in the mean-field value $|\Delta_{MF}(r)|$ could be large. As a consequence, due to large spatial variations, fluctuation effects become crucial in the regions where $\Delta(r)$ is small. Of these, the most important are the thermal fluctuations in the *phase* of the order parameter $\varphi(r)$. In this case, the fluctuations in the phase of the order parameter in mesoscopic "islands" prevent long-range superconductivity, i.e., the global critical temperature T_C is determined by the global phase coherency, whereas the pair condensate could exist well above T_C.[19,20] The experimental results shown in Fig. 8 support the picture in which, at $T > T_C$, metastable superconducting islands of nonzero order parameter are frozen, while the long-range coherence associated with a bulk superconducting state is prevented by thermal fluctuations in the phase.

The important consequence of the presence of the Cooper pair fluctuation above T_C is the appearance of a so-called pseudogap,[19,24,55] i.e., decreasing of the one-electron density of states near the Fermi level. In particular, according to one point of view,[19,23,25] in the pseudogap state high-T_C cuprates could be considered as an unconventional metal, i.e., as a SC that has lost its phase rigidity due to phase fluctuations. A large pseudogap is indeed detected in numerous experiments on manganites,[33] and it may be suggested that at least a portion of the observed pseudogap value is due to pairing without global phase coherency. A precursor diamagnetism above T_C provides additional arguments for survival of the pair condensate well above T_C in cuprates[26,28] as well as in disordered MgB_2,[56] and in oxypnictides.[57] However, for manganites, this kind of response may be strongly suppressed by ferromagnetic order of the localized moments and the spin-triplet state of the condensate.

At the end of this section, let us briefly discuss another possible explanation which may be related to our observations [for more extended discussion the reader is referred to Ref. 30(b)]. It was predicted that in *s*-wave SC/F structures, so-called odd-frequency pairing could take place.[13] In this case, the Cooper pair wave function is symmetric under exchange of spatial and spin coordinates, but antisymmetric under exchange of time coordinates. However, for odd-frequency *s*-wave spin-triplet pairing the *static* gap is zero. We observe a nonzero gap magnitude, and thus, in our opinion, this mechanism[13] of the proximity effect is not related to our case. A giant proximity effect (a logarithmic dependence of the junction critical temperature on the junction width) was predicted for a tunnel junction of two SCs with the barrier formed by a SC that has lost its phase rigidity due to phase fluctuations.[58] We think that to a certain extent this scenario[58] of the proximity effect could be relevant to our case.

V. SUMMARY

Summarizing, to study the phenomenon of the unconventional mutual influence of singlet *s*-wave superconducting pairing and the non-Fermi half-metallic ferromagnetic state of doped manganites found in Refs. 29 and 30, we prepared MgB_2–(nano) $La_{0.67}Sr_{0.33}MnO_3$ composites. Superconductivity of samples of MgB:LSMO with 3:1 and 4:1 weight ratios was observed. A few features have been detected for the bulk sample characteristics which, in our opinion, can hardly be explained within the framework of the conventional percolation model. Using point contact spectroscopy, three distinct quasiparticle energy gaps $\Delta_1(\pi)$, $\Delta_2(\sigma)$, and Δ_{tr} were clearly revealed. Two of these gaps were identified as enhanced gaps in the quasiparticle spectrum of the MgB_2 in the composite; the third gap Δ_{tr} was the same as those earlier detected in PCs of (La,Sr)MnO_3 and (La,Ca)MnO_3 with Pb or MgB_2. A noteworthy argument is the temperature behavior of the Δ_{tr} gap, which does not follow the BCS dependence. Andreev reflection spectroscopy on PCs between the samples and half-metallic $La_{0.65}Ca_{0.35}MnO_3$ electrodes provides additional evidence in favor of an unconventional superconducting state in the MgB:LSMO composite.

In our opinion, the results obtained testify to a type of superconducting proximity effect which provides for phase-coherency stiffness. Specifically, at low temperature in a half-metallic ferromagnetic state of (La,Sr)MnO_3, phase-incoherent superconductivity (a local triplet pairing condensate) exists. However, although the local gap amplitude is large, there is no phase stiffness and the system is incapable of displaying a long-range superconducting response. Nonetheless, local phase rigidity survives. Being proximity coupled to MgB_2, the long-range coherency is restored. Inversely, the manganite in a superconducting state with large energy pairing, due to the proximity effect, enhances the MgB_2 superconducting state. That is, here we deal with some kind of "mutual" proximity effect. Yet further experiments are definitely needed in order to prove (or disprove) this scenario and understand the mechanism causing the local triplet pairing in doped manganites.

Finally, designing ways to raise the superconducting transition temperature has always been an important goal of condensed matter research. Many believe (see, e.g., Refs. 19 and 27) that some compounds should be very high-temperature SCs. These materials will play crucial roles for both fundamental science and applications. Specifically, so-called superconducting spintronics[59,60] is one of the most attractive areas of spintronics, and requires a class of superconducting materials with spin-polarized transport. Our results demonstrate that an effective source of a spin-polarized supercurrent can be designed using nanogranular manganites and a conventional *s*-wave SC. Also, elucidation of the origin of the latent high-T_C superconductivity in doped manganites will likely be a crucial step in our progress towards understanding the physics of this family of compounds.

ACKNOWLEDGMENTS

The authors acknowledge I. Danilenko and O. Gorban' for the preparation of manganite and magnetite nanoparticles. We also are grateful to M. Kupriyanov, Ya. Fominov, E. Pashitskii, S. Ryabchenko, A. D'yachenko, V. Loktev, A. Omelyanchouk, and M. Belogolovskii for useful discussions.

[1] A. I. Buzdin, Rev. Mod. Phys. **77**, 935 (2005).
[2] M. Giroud, H. Courtois, K. Hasselbach, D. Mailly, and B. Pannetier, Phys. Rev. B **58**, R11872 (1998).
[3] V. T. Petrashov, I. A. Sosnin, I. Cox, A. Parsons, and C. Troadec, Phys. Rev. Lett. **83**, 3281 (1999).
[4] M. D. Lawrence and N. Giordano, J. Phys.: Condens. Matter **11**, 1089 (1999).
[5] V. Peňa, Z. Sefrioui, D. Arias, C. Leon, J. Santamaria, M. Varela, S. J. Pennycook, and J. L. Martinez, Phys. Rev. B **69**, 224502 (2004).
[6] I. Sosnin, H. Cho, V. T. Petrashov, and A. F. Volkov, Phys. Rev. Lett. **96**, 157002 (2006).
[7] R. S. Keizer, S. T. B. Goennenwein, T. M. Klapwijk, G. Maio, G. Xiao, and A. Gupta, Nature (London) **439**, 825 (2006).
[8] T. S. Khaire, M. A. Khasawneh, W. P. Pratt, Jr., and N. O. Birge, Phys. Rev. Lett. **104**, 137002 (2010).
[9] J. Wang, M. Singh, M. Tian, N. Kumar, B. Liu, C. Shi, J. K. Jain, N. Samarth, T. E. Mallouk, and M. H. W. Chan, Nat. Phys. **6**, 389 (2010).
[10] Y. Kalcheim, O. Millo, M. Egilmez, J. W. A. Robinson, and M. G. Blamire, Phys. Rev. B **85**, 104504 (2012).
[11] C. Klose, T. S. Khaire, Yixing Wang, W. P. Pratt, Jr., N. O. Birge, B. J. McMorran, T. P. Ginley, J. A. Borchers, B. J. Kirby, B. B. Maranville, and J. Unguris, Phys. Rev. Lett. **108**, 127002 (2012).
[12] A. Kadigrobov, R. I. Skekhter, and M. Jonson, Europhys. Lett. **54**, 394 (2001).
[13] F. S. Bergeret, A. F. Volkov, and K. B. Efetov, Phys. Rev. Lett. **86**, 4096 (2001); Rev. Mod. Phys. **77**, 1321 (2005).
[14] M. Eschrig, J. Kopu, J. C. Cuevas, and G. Schön, Phys. Rev. Lett. **90**, 137003 (2003); M. Eschrig and T. Löfwander, Nat. Phys. **4**, 138 (2008).
[15] D. A. Ivanov, Ya. V. Fominov, M. A. Skvortsov, and P. M. Ostrovsky, Phys. Rev. B **80**, 134501 (2009).
[16] G. Deutscher, in *Percolation, Localization and Superconductivity*, edited by A. B. Goldman and S. A. Wolf (Plenum, New York, 1984), p. 95; M. A. Skvortsov, A. I. Larkin, and M. V. Feigel'man, Phys. Rev. Lett. **92**, 247002 (2004); I. S. Beloborodov, K. B. Efetov, A. V. Lopatin, and V. M. Vinokur, Phys. Rev. B **71**, 184501 (2005).
[17] M. A. Skvortsov, A. I. Larkin, and M. V. Feigel'man, Usp. Fiz. Nauk (Suppl.) **171**, 76 (2001).
[18] I. Sternfeld, V. Shelukhin, A. Tsukernik, M. Karpovski, A. Gerber, and A. Palevski, Phys. Rev. B **71**, 064515 (2005).
[19] V. J. Emery and S. A. Kivelson, Phys. Rev. Lett. **74**, 3253 (1995); V. J. Emery, S. A. Kivelson, and O. Zachar, Phys. Rev. B **56**, 6120 (1997).
[20] E. Berg, D. Orgad, and S. A. Kivelson, Phys. Rev. B **78**, 094509 (2008).
[21] M. Chand, M. Mondal, A. Kamlapure, G. Saraswat, A. Mishra, J. Jesudasan, V. C. Bagwe, S. Kumar, V. Tripathi, L. Benfatto, and P. Raychaudhuri, J. Phys.: Conf. Ser. **273**, 012071 (2011).
[22] A. Glatz, A. A. Varlamov, and V. M. Vinokur, Phys. Rev. B **84**, 104510 (2011).
[23] Y. J. Uemura, G. M. Luke, B. J. Sternlieb *et al.*, Phys. Rev. Lett. **62**, 2317 (1989).
[24] V. M. Loktev, R. M. Quick, and S. G. Sharapov, Phys. Rep. **349**, 1 (2001).
[25] J. L. Tallon, J. W. Loram, J. R. Cooper, C. Panagopoulos, and C. Bernhard, Phys. Rev. B **68**, 180501(R) (2003).
[26] L. Li, Y. Wang, S. Komiya, S. Ono, Y. Ando, G. D. Gu, and N. P. Ong, Phys. Rev. B **81**, 054510 (2010).
[27] L. S. Bilbro, R. V. Aguilar, G. Logvenov, O. Pelleg, I. Bozovic, and N. P. Armitage, Nat. Phys. **7**, 298 (2011).
[28] J. Mosqueira, J. D. Dancausa, and F. Vidal, Phys. Rev. B **84**, 174518 (2011).
[29] V. N. Krivoruchko, V. Yu. Tarenkov, A. I. D'yachenko, and V. N. Varyukhin, Europhys. Lett. **75**, 294 (2006).
[30] V. N. Krivoruchko and V. Yu. Tarenkov, Phys. Rev. B **75**, 214508 (2007); **78**, 054522 (2008).
[31] Y. G. Naidyuk and I. K. Yanson, *Point-Contact Spectroscopy*, Springer Series in Solid State Science, Vol. 145 (Springer, Berlin, 2004).
[32] X. X. Xi, Rep. Prog. Phys. **71**, 116501 (2008).
[33] E. Dagotto, T. Hotta, and A. Moreo, Phys. Rep. **344**, 1 (2001).
[34] M. M. Savosta, V. N. Krivoruchko, I. A. Danielenko, V. Yu. Tarenkov, T. E. Konstantinova, A. V. Borodin, and V. N. Varyukhin, Phys. Rev. B **69**, 024413 (2004); V. Krivoruchko, T. Konstantinova, A. Mazur, A. Prokhorov, V. Varyukhin, J. Magn. Magn. Mater. **300**, e122 (2006).
[35] A. S. Mazur, V. N. Krivoruchko, and I. A. Danilenko, Low Temp. Phys. **33**, 931 (2007).
[36] D. C. Larbalestier, L. D. Cooley, M. O. Rikel, A. A. Polyanskii, J. Jiang, S. Patnaik, X. Y. Cai, D. M. Feldmann, A. Gurevich, A. A. Squitieri, M. T. Naus, C. B. Eom, E. E. Hellstrom, R. J. Cava, K. A. Regan, N. Rogado, M. A. Hayward, T. He, J. S. Slusky, P. Khalifah, K. Inumaru, and M. Haas, Nature (London) **410**, 186 (2001).
[37] Yi Bing Zhang, Di Fan Zhou, Zhen Xing Lv, Zhen Yan Deng, Chuan Bing Cai, and Shi Ping Zhou, J. Appl. Phys. **107**, 123907 (2010).
[38] Yu. V. Sharvin, Sov. Phys. JETP **21**, 655 (1965).
[39] A. I. D'yachenko, V. A. D'yachenko, V. Yu. Tarenkov, and V. N. Krivoruchko, Fiz. Tverd. Tela (St. Peterburg) **48**, 407 (2006) [Phys. Solid. State **48**, 432 (2006)].
[40] I. Leonov, A. N. Yaresko, V. N. Antonov, and V. I. Anisimov, Phys. Rev. B **74**, 165117 (2006).
[41] Yu. S. Dedkov, U. Rüdiger, and G. Güntherodt, Phys. Rev. B **65**, 064417 (2002).
[42] P. Y. Song, J. F. Wang, C. P. Chen, H. Deng, and Y. D. Li, J. Appl. Phys. **100**, 044314 (2006).
[43] M. Kasai, T. Ohno, Y. Kanke, Y. Kozono, M. Hanazono, and Y. Sugita, Jpn. J. Appl. Phys. **29**, L2219 (1990).
[44] M. Kasai, Y. Kanke, T. Ohno, and Y. Kozono, J. Appl. Phys. **72**, 5344 (1992).
[45] R. C. Dynes, V. Narayanamurti, and J. P. Garno, Phys. Rev. Lett. **41**, 1509 (1978).
[46] I. I. Mazin, O. K. Andersen, O. Jepse, O. V. Dolgov, J. Kortus, A. A. Golubov, A. B. Kuz'menko, and D. van der Marel, Phys. Rev. Lett. **89**, 107002 (2002).
[47] A. F. Andreev, Sov. Phys. JETP **19**, 1228 (1964).
[48] G. E. Blonder, M. Tinkham, and T. M. Klapwijk, Phys. Rev. B **25**, 4515 (1982).
[49] D. Daghero and R. S. Gonnelli, Supercond. Sci. Technol. **23**, 043001 (2010).
[50] W. E. Pickett and D. J. Singh, Phys. Rev. B **53**, 1146 (1996); J. Y. T. Wei, N.-C. Yeh, and R. P. Vasquez, Phys. Rev. Lett. **79**, 5150 (1997); M.-H. Jo, N. D. Mathur, N. K. Todd, and M. G. Blamire, Phys. Rev. B **61**, 14905(R) (2000).
[51] M. Hurd, S. Datta, and P. F. Bagwell, Phys. Rev. B **54**, 6557 (1996).
[52] B. A. Aminov, A. A. Golubov, and M. Yu. Kupriyanov, Phys. Rev. B **53**, 365 (1996).

[53]A. Brinkman, A. A. Golubov, and M. Yu. Kupriyanov, Phys. Rev. B **69**, 214407 (2004).
[54]T. Tokuyasu, J. A. Sauls, and D. Rainer, Phys. Rev. B **38**, 8823 (1988).
[55]M. Norman, D. Pines, and C. Kallin, Adv. Phys. **54**, 715 (2005).
[56]E. Bernardi, A. Lascialfari, A. Rigamonti, and L. Romano, Phys. Rev. B **77**, 064502 (2008).
[57]G. Prando, A. Lascialfari, A. Rigamonti, L. Romanò, S. Sanna, M. Putti, and M. Tropeano, Phys. Rev. B **84**, 064507 (2011).
[58]D. Marchand, L. Covaci, M. Berciu, and M. Franz, Phys. Rev. Lett. **101**, 097004 (2008).
[59]S. Anders, M. G. Blamire, F.-Im. Buchholz *et al*., Physica C **470**, 2079 (2010).
[60]Y. C. Tao and J. G. Hu, J. Appl. Phys. **107**, 041101 (2010).